



Toward a warmer Arctic Ocean: Spreading of the early 21st century Atlantic Water warm anomaly along the Eurasian Basin margins

Igor A. Dmitrenko,^{1,2} Igor V. Polyakov,¹ Sergey A. Kirillov,³ Leonid A. Timokhov,³ Ivan E. Frolov,³ Vladimir T. Sokolov,³ Harper L. Simmons,¹ Vladimir V. Ivanov,¹ and David Walsh⁴

Received 9 February 2007; revised 27 November 2007; accepted 21 December 2007; published 17 May 2008.

[1] We document through the analysis of 2002–2005 observational data the recent Atlantic Water (AW) warming along the Siberian continental margin due to several AW warm impulses that penetrated into the Arctic Ocean through Fram Strait in 1999–2000. The AW temperature record from our long-term monitoring site in the northern Laptev Sea shows several events of rapid AW temperature increase totaling 0.8°C in February–August 2004. We hypothesize the along-margin spreading of this warmer anomaly has disrupted the downstream thermal equilibrium of the late 1990s to earlier 2000s. The anomaly mean velocity of $2.4\text{--}2.5 \pm 0.2$ cm/s was obtained on the basis of travel time required between the northern Laptev Sea and two anomaly fronts delineated over the Eurasian flank of the Lomonosov Ridge by comparing the 2005 snapshot along-margin data with the AW pre-1990 mean. The magnitude of delineated anomalies exceeds the level of pre-1990 mean along-margin cooling and rises above the level of noise attributed to shifting of the AW jet across the basin margins. The anomaly mean velocity estimation is confirmed by comparing mooring-derived AW temperature time series from 2002 to 2005 with the downstream along-margin AW temperature distribution from 2005. Our mooring current meter data corroborate these estimations.

Citation: Dmitrenko, I. A., I. V. Polyakov, S. A. Kirillov, L. A. Timokhov, I. E. Frolov, V. T. Sokolov, H. L. Simmons, V. V. Ivanov, and D. Walsh (2008), Toward a warmer Arctic Ocean: Spreading of the early 21st century Atlantic Water warm anomaly along the Eurasian Basin margins, *J. Geophys. Res.*, 113, C05023, doi:10.1029/2007JC004158.

1. Introduction and Motivation

[2] Warm and salty Atlantic Water (AW) plays a special role in the thermal balance of the Arctic Ocean. It enters the Arctic Ocean by two major inflows through Fram Strait and the Barents Sea shelf, merging just north of the Kara Sea [Aagaard, 1989; Rudels *et al.*, 1994] (Figure 1). The merged AW branches sink to an intermediate (150–900 m) level and mix vigorously, following the Eurasian Basin bathymetry in a cyclonic sense as a narrow topographically trapped boundary current with an annual mean speed of 1–5 cm/s [Timofeev, 1957; Woodgate *et al.*, 2001; Karcher *et al.*, 2003; Polyakov *et al.*, 2005]. Near the Lomonosov Ridge the middepth AW flow splits, with part turning northward and following the Lomonosov Ridge, and another part entering the Canada Basin [Aagaard, 1989; Rudels *et al.*, 1994] (Figure 1). During AW transit along the

Eurasian Basin margins, the long-term mean AW core temperature (AWCT) decreases from 2.5 to 3.0°C near Svalbard down to 2.0–2.5°C northward of Franz Josef Land, 1.5°C along the western Laptev Sea continental margin, 1°C northward of New Siberian Islands, and 0.8°C along the Lomonosov Ridge [Timofeev, 1957; Polyakov *et al.*, 2003b] (see also Figure 2a); this decrease provides evidence that some fraction of the AW heat is lost during downstream propagation due to lateral and vertical heat exchange.

[3] Over the past several decades the AW temperature has exhibited substantial variability. Shifts in atmospheric circulation patterns have resulted in increased transport and temperature of AW entering the Arctic via Fram Strait [Rudels *et al.*, 2000]. The first evidence of strong warming within the AW layer was found in the Nansen Basin in 1990 [Quadfasel *et al.*, 1991]. Positive AW anomalies of up to 1°C were carried along the continental margins into the Arctic Ocean interior [Woodgate *et al.*, 2001; Schauer *et al.*, 2002]. Polyakov *et al.* [2004] found that the 1990s maximum fits well with a recurring pattern of multidecadal AW variability that occurs over a timescale of 50–80 years.

[4] This study was motivated by recent reports [Schauer *et al.*, 2004; Polyakov *et al.*, 2005] that since the late 1990s, AW temperature has shown a new tendency to increase. Our

¹International Arctic Research Center, University of Alaska Fairbanks, Fairbanks, Alaska, USA.

²Now at Leibniz Institute of Marine Sciences at the University of Kiel, Kiel, Germany.

³Arctic and Antarctic Research Institute, St. Petersburg, Russia.

⁴Pacific Tsunami Warning Center, Ewa Beach, Hawaii, USA.

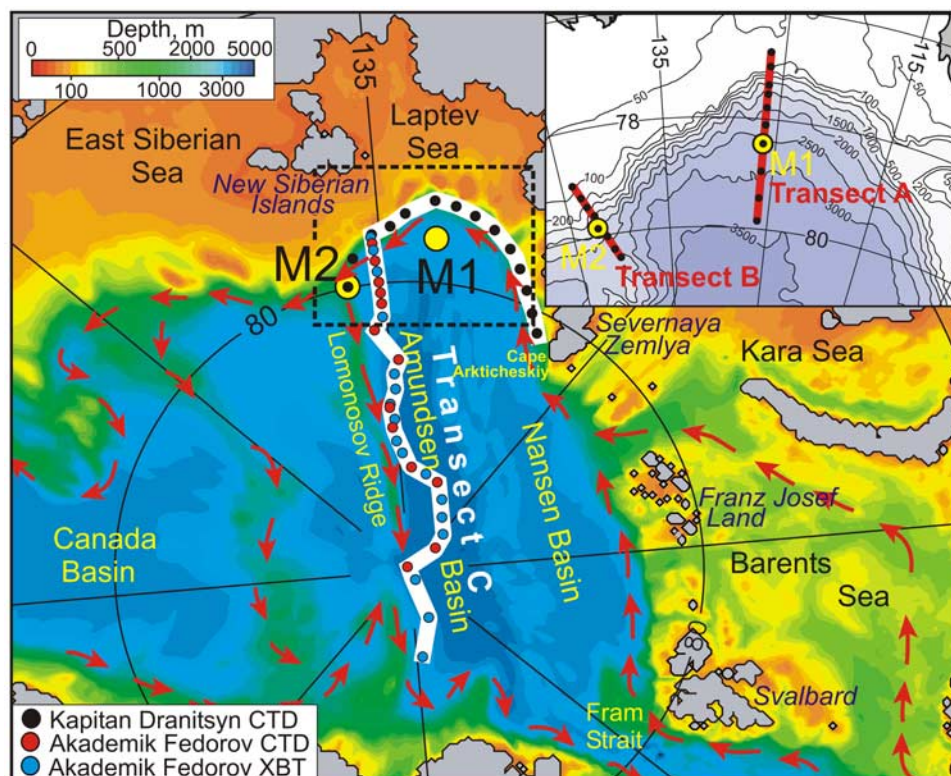


Figure 1. A map of the Arctic Ocean with inset showing an enlarged view of the northern Laptev Sea region (dashed square). Red arrows trace the AW pathways. Yellow circles mark the mooring positions. White line shows along-margin CTD/XBT Transect C occupied in August–September 2005. Inset shows CTD cross-margin transects A and B (red lines) carried out in 2002–2005. Bathymetry is adapted from the International Bathymetric Chart of the Arctic Ocean (IBCAO), 2001 version.

data indicate that over the Eurasian Basin margins the Arctic Ocean exhibits sharp frontal features suggestive of downstream along-margin propagation of several warm AW impulses. Section 2 summarizes the data set used in this study. Section 3 draws a picture of the AW pre-1990 mean over the Eurasian Basin composed using the hydrographic historical data of 1890–1990. Through the analysis of 2002–2005 observational data, section 4 documents the recent AW warming along the Siberian shelf margin. Section 5 compares the AW pre-1990 mean drawn in section 3 with the 2005 along-margin hydrographic data. Following *Swift et al.* [1997], we suggest that the AW warmer anomalies over sloping topography are the tracers that are carried along by the boundary current. We delineate the anomaly fronts and hypothesize that the along-margin spreading of the new AW warm anomaly is disrupting the downstream thermal equilibrium of the late 1990s to earlier 2000s, when the previous sustained warming of the AW layer had disappeared from the Barents and Laptev seas slope, presumably having been advected farther downstream [*Boyd et al.*, 2002; *Morison et al.*, 2002; *Polyakov et al.*, 2003a], and the intermediate water layer relaxed toward the climatic mean conditions [*Morison et al.*, 2006]. Section 6 reveals the AW propagation speed that provides the best match between the mooring temperature time series of 2002–2005, and the downstream along-margin temperature section of summer 2005. Section 7 combines our inferences to estimate the anomaly propagation speed, calculating the anomaly travel time from the Laptev Sea

long-term monitoring site to the location of the anomaly front delineated by comparison of 2005 along-margin data with the AW pre-1990 mean and the mooring record. Finally, we verify these estimations using our mooring current meter data, numerical modeling by *Karcher et al.* [2003], and tracer analysis by *Frank et al.* [1998].

2. Data

[5] The data used in this study were collected from two moorings deployed offshore of the Laptev Sea continental slope (Figure 1). Mooring M1 ($78^{\circ}26'N$, $125^{\circ}37'E$) collected data during three consecutive years (2002–2003, 2003–2004, and 2004–2005). The mooring was equipped with a McLane Moored Profiler (MMP), an instrument that samples an underwater vertical profile along a mooring line at a speed of about 25 cm/s, with a sampling period of 0.5 s. The MMP was equipped with a CTD (conductivity, temperature, and depth) meter manufactured by Falmouth Scientific, Inc. (FSI) in 2002–2004 or Sea-Bird Electronics, Inc. (SBE) in 2004–2005, and an ACM (acoustic current meter), giving measurements of velocity and manufactured by FSI. During the first year the profiler was programmed to profile between target depths of 164 and 2607 dbar. Drive motor spring failure and ballasting problems resulted in a gradual decrease in profiling range over the course of the year. The MMP finally stopped profiling in February 2003 at a depth of 435 dbar. Because of technical problems no reliable current records were obtained during the first year. The

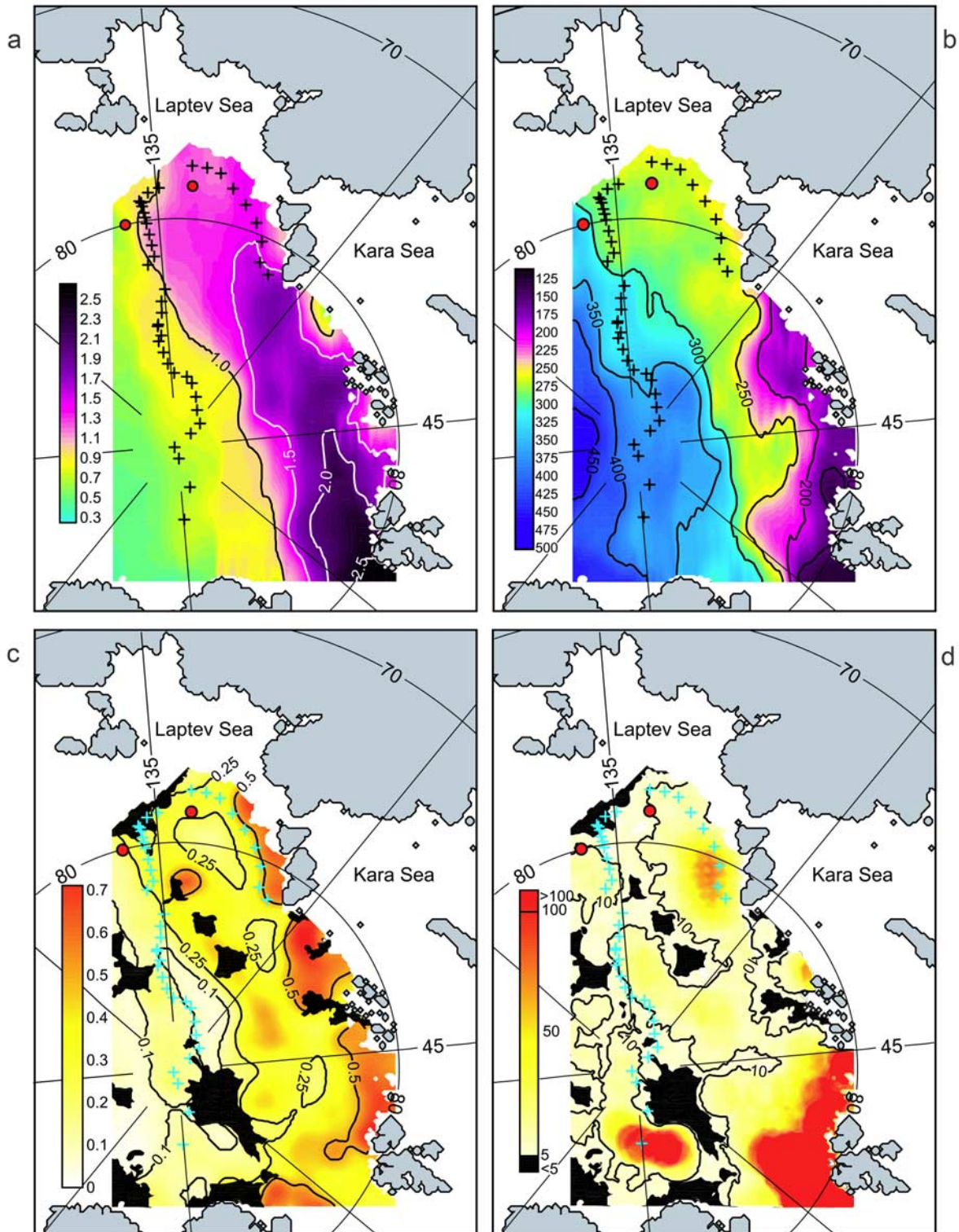


Figure 2. The gridded long-term (1894–1990) mean (a) AWCT ($^{\circ}\text{C}$), (b) AW core depth (m), (c) the AWCT standard deviation, and (d) the number of stations occupied between 1894 and 1990. Red dots and blue or black crosses show 2002–2005 moorings and 2005 CTD/XBT stations, respectively. Black patches mark areas within which fewer than 5 measurements were made.

second-year deployment provided yearlong CTD and velocity records between 105 and 1509 dbar. The third-year deployment provided reliable CTD and current records between 90 and 900 dbar until 20 February 2005. After that date, ballasting problems resulted in a gradual sinking of the MMP from the lower target depth of 900 dbar down to the bumper depth of 1880 dbar. The upward looking Teledyne RD Instruments (RDI) 300 kHz Workhorse Sentinel Acoustic Doppler Current Profiler (ADCP) placed in 2004–2005 at a depth of 54.5 dbar captured water properties above the AW layer defined by the 0°C isotherm (note that under this definition the cooler AW entering the Arctic Ocean through the northern Kara Sea would no longer be identified as AW). However, the velocity record from the lower ADCP bin (48.5 dbar) was employed for comparison with the upper level MMP velocity record for verification of the MMP ACM velocity sensor only.

[6] The conventional mooring M2 (79°55'N, 142°21'E, Figure 1) collected data from September 2004 to September 2005. It was equipped with an upward looking RDI 300 kHz Workhorse Sentinel ADCP placed at a depth of 132 dbar, two Aanderaa Instruments Recording Current Meters (RCM 11s) (254 and 826 dbar), and four SBE-37s, three with conductivity and temperature (CT) sensors (40, 133, and 253 dbar), and one with a CTD sensor (297 dbar). ADCP velocity data were acquired throughout the year between 42 and 126 dbar at 4 m depth intervals, with a 60-min ensemble time interval and 60 pings per ensemble. CT, CTD, and current meters provided 60-min interval (RCM 11s) and 30-min interval (SBE-37s) yearlong records of velocity, conductivity, temperature, and pressure at fixed depths with a sampling period of 1 h (RCM 11s) and 15 min (SBE-37s). The SBE-37 CT at 133 dbar was located near the upper boundary of the AW layer, while the deeper SBE-37s measured positive temperatures throughout the year. The SBE-37 at a depth of 40 dbar was located in the upper mixed layer and data from that instrument were not considered in this analysis.

[7] Mooring observations were complemented by oceanographic transects across the Laptev Sea continental slope (transects A and B, Figures 1 and 5) occupied during icebreaker *Kapitan Dranitsyn* cruises in September 2002–2005 using a shipboard SBE19+ CTD. In addition, the oceanographic transect along the Laptev Sea continental slope approximately following the 1500 m depth contour was carried out in September 2005. It was complemented by an oceanographic transect approximately along the Eurasian flank of the Lomonosov Ridge occupied by a shipboard SBE-911 CTD and Lockheed Martin Sippican Expendable Bathythermographs (XBTs) (Transect C, Figures 1 and 6a) during the August–September 2005 cruise of the R/V *Akademik Fedorov*. Individual temperature and conductivity measurements are accurate to $\pm 0.005^\circ\text{C}$ and $\pm 0.0005\text{ S/m}$, respectively, for the SBE-19+, and $\pm 0.001^\circ\text{C}$ and $\pm 0.0003\text{ S/m}$ for the SBE-911. XBT accuracy is $\pm 0.05^\circ\text{C}$. At the M1 mooring, the MMP carried an FSI micro-CTD sensor (2002–2004) and an SBE 41CP CTD sensor (2004–2005) with temperature and conductivity measurement accuracies of $\pm 0.002^\circ\text{C}$ and $\pm 0.0002\text{ S/m}$, respectively. The MMP ACM current velocity precision and resolution are reported to be $\pm 3\%$ of reading and $\pm 0.01\text{ cm/s}$, respectively. Compass accuracy is $\pm 2^\circ$. RCM 11 Doppler Current

Sensor precision and resolution are reported to be $\pm 1\%$ of reading and $\pm 0.3\text{ cm/s}$, respectively. Compass accuracy is $\pm 5^\circ$. RDI ADCP precision and resolution are $\pm 0.5\%$ and $\pm 0.1\text{ cm/s}$, respectively. Compass accuracy is similar to that of the RCM 11.

3. The Atlantic Water Long-Term Mean Over the Eurasian Basin

[8] The AW long-term mean used in this study has been compiled primarily in order to estimate the mean AW cooling along the Eurasian continental margin for comparison with the 2005 along-margin CTD/XBT data. The AW warming of the 1990s would bias the estimate of long-term mean cooling of AW along the margin. Therefore all post-1990 data were eliminated from our historical hydrographic data set that consolidates different data sets from 1894 to 1990 previously used by *Polyakov et al.* [2003b, 2004] and for the *Environmental Working Group* [1997] atlas of the Arctic Ocean. While the first oceanographic observations in the Arctic Ocean deep-sea area between 90°E and 150°E were made by Nansen in 1894–1895, the systematic oceanographic observations in this area began only in the 1930s (67 stations), when Russians started the ice drift stations monitoring program. After a gap in the 1940s (10 stations), in the 1950s the first Soviet basin-scale aircraft surveys were conducted (51 stations). A few observations are available from the 1960s (32 stations), but the 1970s was an exceptional period with seven Soviet aircraft surveys from 1973 to 1979 (204 stations). Most measurements in the 1980s (155 stations) were made within the limited area off the Severnaya Zemlya Islands (Figure 2d). Summarizing this short description of our historical data set, one may conclude that the most of our data came from the 1950s–1970s when the AW layer was relatively cold [see *Polyakov et al.*, 2004, Figure 2, top]. The spatial distribution of the individual (snapshot) measurements interpolated in a regular 30 km grid over the 150 km search radius is shown in Figure 2d.

[9] The long-term mean AWCT (T) (Figure 2a) is defined as the maximum temperature between the AW layer boundaries (defined by the 0°C isotherms) averaged first by decade, and then over the whole period of 1894–1990 in a regular 30 km grid over the 150 km search radius. Areas shallower than 500 m have been omitted. Despite the coarse vertical resolution of the historical data in the vicinity of the AW core, the AWCT can be computed quite accurately, although the precise depth of temperature maximum (Figure 2b) cannot be accurately deduced from most of the data that are available before the 1990s [*Polyakov et al.*, 2003b]. The long-term mean AWCT standard deviation δT is shown in Figure 2c. Note that the δT was computed using all data prior to 1990 with no decadal subdivision.

[10] The AW pre-1990 mean (Figure 2) demonstrates cyclonic AW inflow around the central deep Arctic Ocean Basin that primarily follows the bottom topography. Over the Eurasian Basin the long-term mean AWCT exhibits substantial spatial variability, gradually decreasing along-margin from 2.5°C in Fram Strait, to 1.50°C near Cape Arkticheskiy, 1.12°C at the M1 mooring position, and 1.0°C over the Eurasian side of the Lomonosov Ridge (Figure 2a). This rate of decrease is in good agreement with earlier

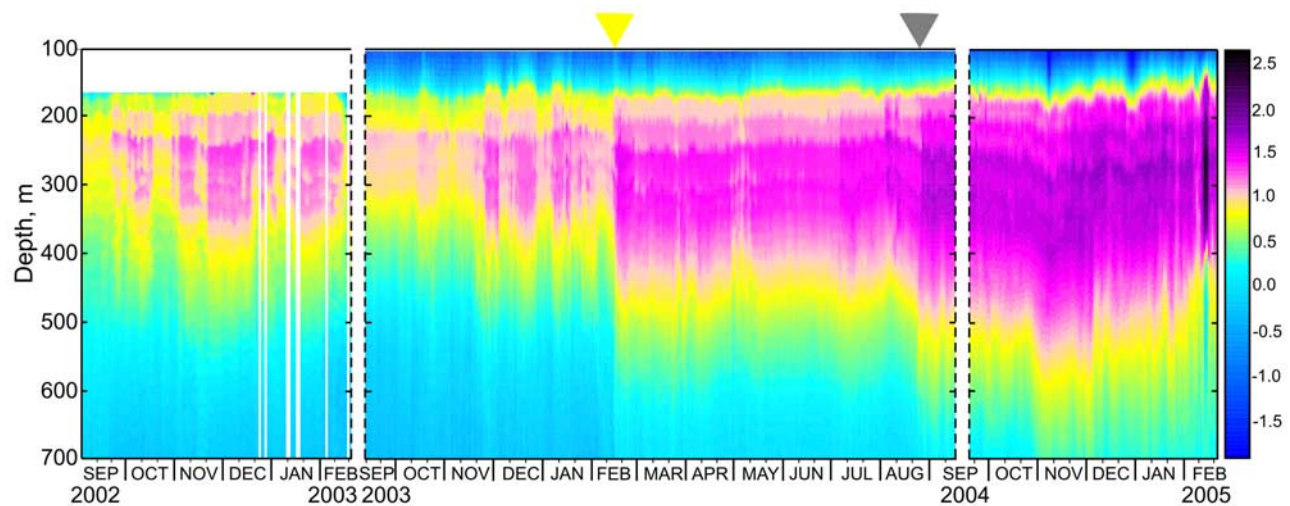


Figure 3. Water temperature ($^{\circ}\text{C}$) from the M1 McLaine Moored Profiler (MMP). Gray and yellow arrows delineate the onset of February and August 2004 AW warmer anomalies, respectively. Blank areas represent missing data. Ten-meter vertical binning is used.

results by *Timofeev* [1957], and with recent data compiled by *Polyakov et al.* [2003b]. Because of insufficient data coverage (Figure 2d) and smoothing procedures our AW mean does not reproduce the bifurcation of the AW boundary current which occurs north of the New Siberian Islands, where one branch of the current follows the Eurasian flank of the Lomonosov Ridge toward the north, while another branch enters the Canada Basin [*Rudels et al.*, 1994; *Woodgate et al.*, 2001; *Schauer et al.*, 2002]. Note, however, that the warmer AW boundary jet over the Eurasian flank of the Lomonosov Ridge has been well confirmed by snapshot measurements taken across the Nansen and Amundsen Basins (for example by *Schauer et al.* [2002]). As it cools, the AW core deepens along-margin, from approximately 100 m north of Svalbard to 250 m near Cape Arkticheskiy, 300 m north of the New Siberian Islands, and 375 m at the North Pole (Figure 2b). The AWCT standard deviation demonstrates a tendency to increase from 0.25°C over the central Nansen Basin to more than 0.5°C toward the basin margins. We assume the cross-margin displacement of the AW boundary jet is a possible explanation for this tendency.

4. Toward a Warmer Arctic Ocean: Results of 2002–2005 Observations Along the Eurasian Basin Margins

[11] Here we document the recent AW warming along the Siberian shelf margin through the analysis of 2002–2005 observational data from moorings and summer snapshot transects.

[12] Our 3-yearlong MMP temperature record from the M1 mooring exhibits substantial AW layer temporal variability. Before February 2004 this variability can be mainly attributed to a seasonal cycle, with AW winter temperatures generally higher than summer temperatures (Figure 3). This variability is generated by the wind-driven seasonal shift of the AW jet toward the slope in winter and away from the slope in summer [*Dmitrenko et al.*, 2006]. Since 14 February 2004 this seasonal pattern has been disrupted by a

warming event that can be clearly seen in the MMP record (Figure 3), when the MMP captured an exceptionally strong warming with an AW temperature increase of about 0.4°C . This warming event has been attributed to downstream propagation of the AW warm anomaly first recorded in the Fram Strait in 1999 [*Schauer et al.*, 2004; *Polyakov et al.*, 2005]. Following this event the AW layer equilibrated at a new warmer state for almost seven months, continuing until a second AW temperature increase of about the same magnitude occurred, which was captured in late August 2004 measurements (Figure 3). Since that time the AW layer temperature does not appear to have varied significantly. However, a continuous gradual temperature increase until November 2004 was accompanied by AW layer thickening, and deepening of the AW core by 55 m. From that time until the end of the observational period in February 2005 the AW layer gradually returned to the conditions of September 2004. Although there is no available record between February and August 2005, the CTD cast taken before mooring recovery reveals a general tendency for the AW layer to return to the initial thermal conditions of September 2004 (Figure 4a).

[13] M2 mooring SBE-37 2004–2005 yearlong fixed-depth records of temperature from the AW layer (253 and 297 dbar, not shown) did not exhibit the substantial warming trend. The CTD casts taken at this mooring position before deployment and after recovery also exhibited no substantial difference (Figure 4b). Instead, from midwinter until midsummer 2005 the AW temperature remained about 0.5°C cooler (not shown).

[14] The M1 mooring 1.5 year mean velocity record below 175 m demonstrates an almost unidirectional flow of 80° aligned along isobaths with a mean speed of 2.2 cm/s (Figure 4a). The slight turn at the 115–175 m layer roughly coincides with the upper depth of the AW layer. The M2 mooring annual mean velocity from the AW core (254 dbar) of 3.0 cm/s is also almost along-slope (74°), while in the upper layer (100–130 dbar) the current strengthens up to 5.0 cm/s and turns in a coastward direction of 132° (Figure 4b).

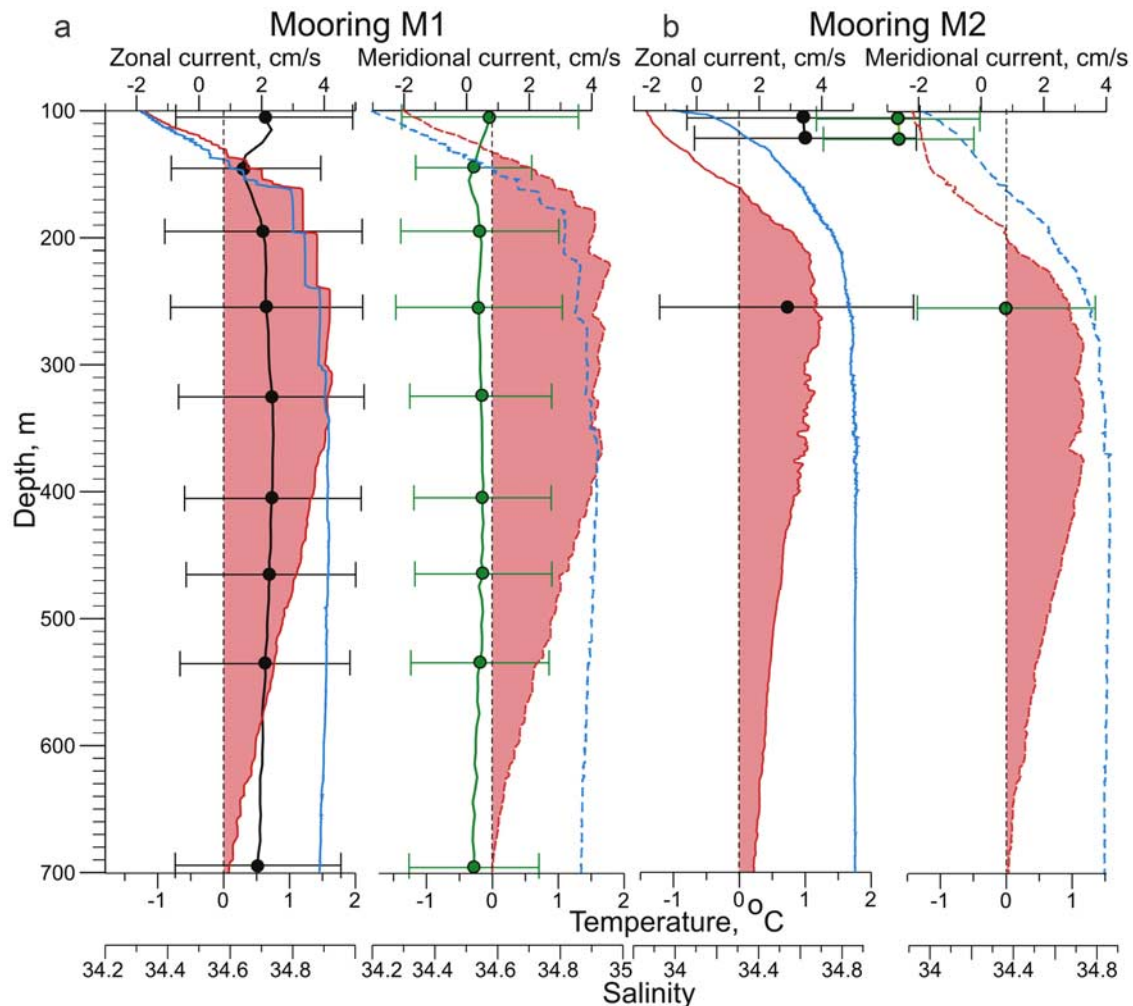


Figure 4. (a) The 1.5-year mean (September 2003 to February 2005) vertical profile of 10-m binned M1 MMP velocity record. (b) Annual mean (September 2004–2005) M2 mooring RCM 11 velocity record at 254 dbar complemented by ADCP 4-m binned annual mean velocity profile at 100–132 dbar. Error bars depict velocity standard deviation at a number of depths. Temperature (red line) and salinity (blue line) profiles taken by shipboard CTD at M1 (Figure 4a) and M2 (Figure 4b) moorings are shown by solid (September 2004) and dashed (September 2005) lines. The AW layer temperature range is shown by the red shaded area.

[15] Annual 2002–2005 cross-margin temperature sections (Figure 5) corroborate our mooring results. Section A taken in 2002 (not shown) and again in 2003 (Figure 5a, top) demonstrates no substantial variability [see also *Dmitrenko et al.*, 2006], while temperature sections A and B occupied in September 2003 and 2004 exhibit dramatically changing AW layer warmth and thickness (Figure 5). At the M1 mooring position the 2004 AW core warming reached 0.7°C. Over the same period of time the AW layer thickened from 325 to 580 m. CTD cross-margin sections occupied in 2003 and 2004 provide further evidence that between 2003 and 2004 the warmer AW anomaly filled the entire northern Laptev Sea. From that time until September 2005 no substantial changes of that range have been observed (Figure 5).

[16] Along the Eurasian Basin margin from Cape Arkticheskiy to the North Pole the AWCT demonstrates substantial spatial variability. The 2005 along-margin

section C shows that the AW core deepens by 110 m from Cape Arkticheskiy to the North Pole (Figure 6a). At the same time, the 2005 AWCT (T^{2005}) shown by the red line in Figure 6b showed spatial variability along transect C as it cooled from 2.2°C down to 1°C. Moreover, the AWCT temperature does not appear to cool gradually, but rather demonstrates spatially nonuniform patterns. Of particular interest is the AWCT cooling from 1.47°C at the intersection of the *Kapitan Dranistin* and *Akademik Fedorov* transects to 1.17°C at the M2 mooring site, while over the same distance toward the North Pole the AWCT exhibits little change. Furthermore, in 2005 the AW core of 1.46°C was found shifted off-slope along transect B (Figure 5b, bottom). This underlies our speculation that the M2 mooring does not accurately capture the AW boundary current which flows farther north and turns along the Lomonosov Ridge before it gets to the M2 mooring position. This conclusion also follows from comparison of vertical CTD profiles taken at

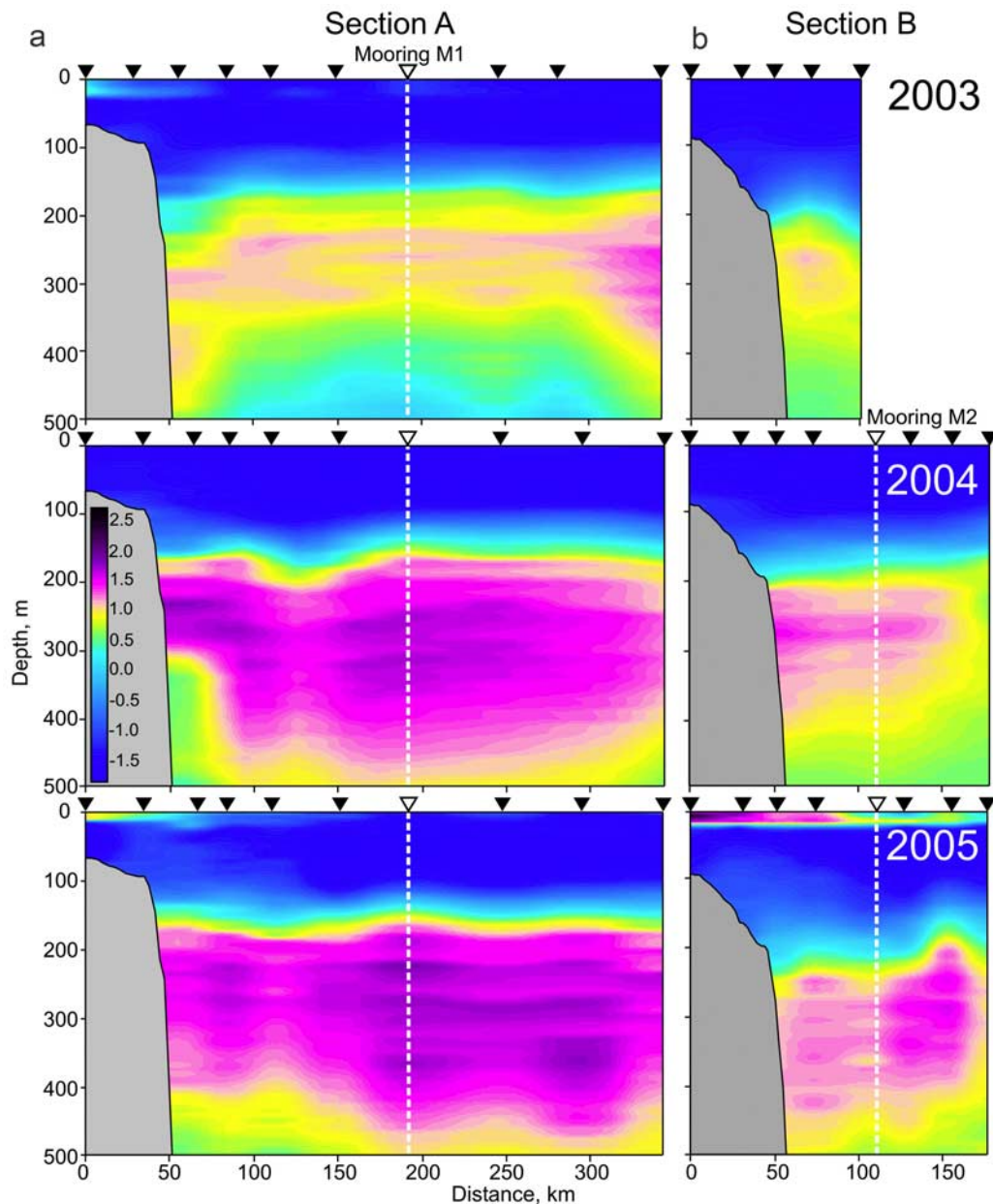


Figure 5. The 10-m binned temperature ($^{\circ}\text{C}$) cross-margin sections (a) A and (b) B taken in September 2003–2005 across the Laptev Sea continental slope. The vertical white dashed line shows mooring positions.

the M1 and M2 moorings (Figure 4). The well-defined temperature-salinity (T-S) structure of thermohaline double-diffusive intrusions within the AW core is considered to be a “marker” for the AW flow [Rudels *et al.*, 1994; Carmack *et al.*, 1997; Rudels *et al.*, 1999; Woodgate *et al.*, 2007]. While the signature of thermohaline intrusions is well defined in the upper AW layer at 150–350 dbar at the M1 position (Figures 3 and 4a), it is suppressed at M2 (Figure 4b).

5. Comparison of the 2005 Along-Margin Transect With Atlantic Water Long-Term Mean

[17] Here we address the causes underlying AWCT spatial variability along the Nansen and Amundsen Basin margins. Swift *et al.* [1997] were the first to infer displace-

ment time of temperature increase in the basin interior due to downstream propagation of the interannual temperature signal in the Fram Strait AW inflow. Following this approach, we argue that a certain fraction of the AW along-margin temperature variability is due to the downstream propagation of two warm AW anomalies that passed the M1 mooring position in February and August 2004 (Figure 3). Our general goal is to delineate the along-margin downstream position of anomaly fronts by comparing the 2005 along-margin CTD/XBT transect with the AW along-margin long-term mean introduced in section 3.

5.1. Approach

[18] Heat lost during the AW transit from Cape Arkticheskiy to the North Pole results in cooling and deepening of the

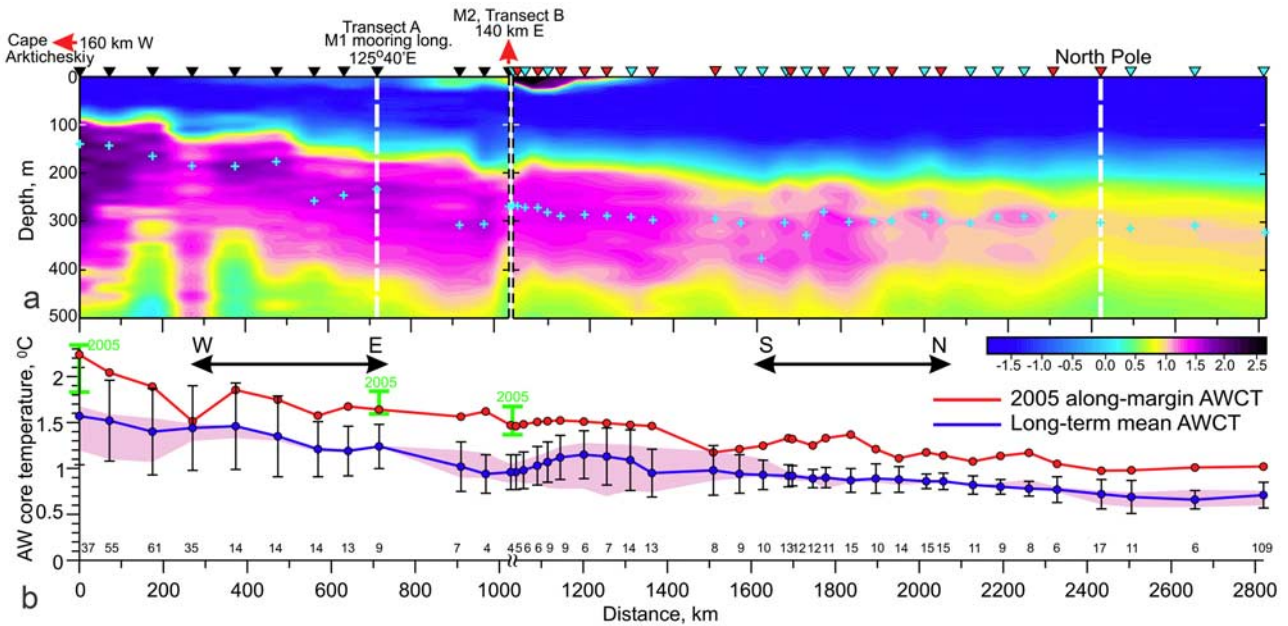


Figure 6. (a) The 10-m binned temperature ($^{\circ}\text{C}$) section C taken in August–September 2005 along the Laptev Sea continental slope (left) and the Eurasian flank of the Lomonosov Ridge (right). Black, red, and blue arrows on the top show the *Kapitan Dranitsyn* CTD, and the *Akademik Fedorov* CTD and XBT stations, respectively. Blue crosses mark the AW core. (b) The 2005 along-margin AWCT (red line), and its long-term mean (blue line). Number of hydrographic stations used for the long-term mean estimations is on the top of bottom axis. The standard deviations of the long-term mean AWCT are shown by black error bars. Green error bars depict the range of 2005 AWCT cross-slope variability derived from 2005 cross-slope sections. Red shading depicts the range of long-term mean AWCT cross-slope variability (see section 5.2 for more detailed explanation).

AW core (Figures 2 and 6a). To be properly detected on a snapshot transect the large-scale thermodynamic warming that is propagating downstream needs to rise above the climatic mean cooling attributed to heat lost along the AW pathways. Furthermore, the AW flows cyclonically into the Arctic Ocean interior with a warm jet migrating from 50 to 300 km off the basin margins [Schauer *et al.*, 2002, Dmitrenko *et al.*, 2006]. Spatial shifting of the AW jet across the basin margins, whether driven by wind, topography, or dynamical instability, produces “noise.” Large-scale thermodynamic warming would need to rise above this level to be detected by a snapshot along-margin transect which does not necessarily follow the AW jet and therefore may contain variability attributed to shifting of the AW jet across the basin margins.

[19] Below we delineate the along-margin position of the AW warm fronts, asking the following questions:

[20] 1. Is the along-margin AW cooling recorded in 2005 affected by downstream propagation of warmer anomalies, i.e., does the magnitude of suspected anomalies exceed the level of climatic mean cooling?

[21] 2. Do these anomalies rise above the level of noise attributed to shifting of the AW jet across the basin margins?

5.2. Definitions

[22] First, we define the long-term mean cooling along the AW pathway from Cape Arkticheskiy to the North Pole using the AW long-term mean compiled in section 3. The long-term mean AWCT T at a number of points i defined in Figure 2 by crosses was taken from the AW pre-1990 mean

shown in Figure 2a. All i points coincide with 2005 CTD/XBT stations. The T_i along-margin regularity is shown in Figure 6b by the blue line. The long-term mean AWCT standard deviation (δT_i) derived from Figure 2c is depicted in Figure 6 by error bars. We retrieve the mean AW jet core temperature (AWJCT) T'_i along a set of cross-margin grid-base-simulated transects defined in the following way. Each transect crosses the along-margin section C roughly perpendicular to C at position i , and extends 150 km in both off-slope and on-slope directions. All regular 30 km grid boxes intersected by transect were counted. Each grid cell represents the averaged individual snapshot measurements over the 150 km radius. Thus each transect encompasses about $18 \cdot 10^4 \text{ km}^2$. The total number of cross-slope snapshot measurements used to compose the individual T'_i data is shown above the bottom axis of Figure 6. The range of the long-term mean AWCT variations along grid-base-simulated cross-slope sections is depicted in Figure 6b by red shading. The maximum AWCT within this range is attributed to the AW jet. The basic regularity of AWJCT spatial variability along transect C provides a background cooling attributed to heat lost from the climatic mean AW jet.

[23] Second, we define the rate of the 2005 AWCT relative to the long-term mean background cooling downstream of the M1 mooring. We assume the 2005 AWCT at the North Pole geographic location ($i = 0$) T_o^{2005} has not yet been affected by the downstream propagation of the new AW anomaly of the early 2000s. The AWCT derived from CTD casts taken in the vicinity of the North Pole throughout the period of 2000–2005 (<http://psc.apl.washington.edu/>

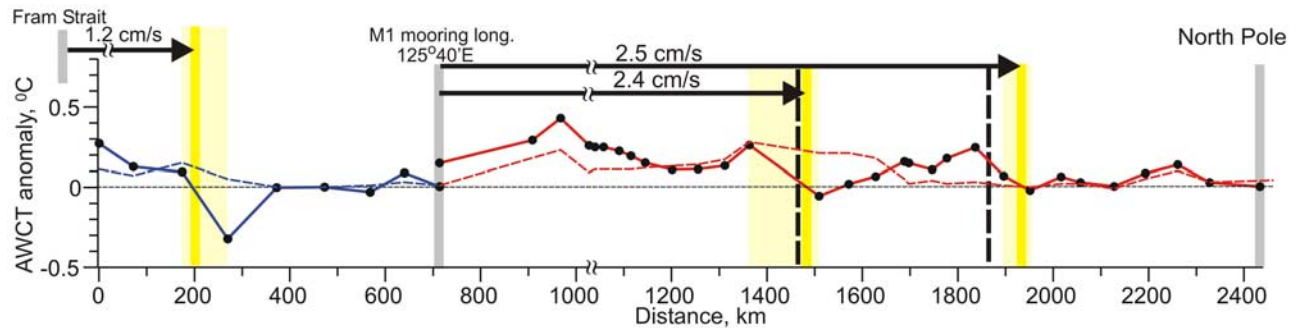


Figure 7. The 2005 AWCT anomaly ($^{\circ}\text{C}$) over along-margin transect C. Red and blue lines show anomaly rate relative to AWJCT long-term mean cooling between the M1 mooring and North Pole and between Cape Arkticheskiy and the M1 mooring, respectively. Dashed line depicts the level of noise (δ) attributed to the cross-margin migration of the AW jet. See text for details of calculating 2005 AWCT anomalies and δ . The vertical yellow lines delineate the suggested AW anomaly fronts attributed to the downstream spreading of two warm AW pulses passing the M1 mooring in February and August 2004 and through Fram Strait in January 2001. Yellow shading shows spatial uncertainty of front determination by nearby oceanographic stations. Black dashed vertical lines delineate the anomaly positions estimated independently from V -lagged correlation between AWCT derived from 2002 to 05 mooring, and 2005 CTD/XBT along-margin records. Numbered arrows show the direction and estimated velocity of anomaly propagation.

northpole/CTDs.html) does not vary significantly, supporting our assumption. However, the September 2005 North Pole AWCT was found to be 0.22°C higher than the long-term mean (Figure 6b). This difference coincides reasonably well with the approximately 0.3°C North Pole AWCT positive anomaly of April 2005, relative to its climatic mean taken from the *Environmental Working Group* [1997] atlas of the Arctic Ocean (<http://psc.apl.washington.edu/northpole/Tslices2005.html>). We speculate that the temperature difference $\Delta_o = T_o^{2005} - T_o'$ between the September 2005 AWCT and the mean AWJCT, both taken at the North Pole location, represents a remnant of the older 1990s anomaly. Therefore, for further comparisons with the 2005 AWCT (T_i^{2005}) the mean AWJCT (T_i') along transect C has been adjusted by Δ_o . Finally, the 2005 AWCT temperature anomaly $\Delta T_i'$ downstream of the M1 mooring is estimated as $\Delta T_i' = T_i^{2005} - (\Delta_o + T_i')$, and is shown in Figure 7 by the red line. The upstream anomaly (blue line in Figure 7) is also defined in this fashion: $\Delta T_i' = T_i^{2005} - (\Delta_{M1} + T_i')$, where $\Delta_{M1} = T_{M1}^{2005} - T_{M1}'$, making the assumption that the meridian at the M1 mooring location has not yet been affected by the warmer AW pulse that passed through Fram Strait in January 2001 [Schauer et al., 2004; Polyakov et al., 2005].

[24] Third, we define the range of noise attributed to the AW jet shifting across the basin margins. To estimate the noise produced by shifting of the AW jet across the basin margins, we take the difference, δ_i , between the long-term mean AWJCT and AWCT, $\delta_i = T_i' - T_i$. When compared with $\Delta T_i'$ (Figure 7), δ_i gives us a basic estimate of what portion of the 2005 AWCT temperature anomaly is due to cross-margin migration of the AW jet.

5.3. Delineation of Along-Margin Atlantic Water Anomaly Fronts

[25] We delineate the along-margin AW anomaly fronts by attributing the spatial irregularity of positive $\Delta T_i'$ values to the downstream progression of warm AW impulses. The

range of estimated 2005 AW anomaly along transect C downstream of the M1 mooring to 1400 km is stably positive, varying between 0.15 and 0.43°C (Figure 7). We may speculate that the rapid drop of $\Delta T_i'$ from 0.26 to -0.06°C between 1350 and 1500 km delineates the first anomaly extension toward the North Pole. However, a different perspective comes from a comparison of anomaly magnitude and noise level δ attributed to the AW jet shifting across the continental margin. Between 700 and 1150 km, where the anomaly magnitude exceeds δ , the mechanism of a shifting jet is only one factor partially contributing to the anomaly estimate. However, the range of δ derived from the 2005 snapshot cross-margin section A (Figure 6, depicted by green error bar) substantially exceeds that of the long-term mean, indicating that for the warmer AW phase cross-slope shifting of the AW jet becomes more significant. Farther north near the suggested anomaly front the noise level δ is relatively high. It is similar to (1100–1300 km) or exceeds (1300–1650 km) the anomaly magnitude, providing evidence that the AW jet shifting across the basin margins is among the potential contributors to the observed $\Delta T_i'$ along-margin variability. The δ range derived from 2005 cross-margin section B corroborates this conclusion. Note that data coverage between 950 km and 1200 km (Figures 2d and 6) is not sufficient to provide a high level of confidence for that interval.

[26] Farther downstream between 1700 and 1900 km the anomaly magnitude increases, considerably exceeding the noise level δ . After reaching a maximum of 0.26°C at 1850 km, at 1940 km it drops down to -0.02°C (Figure 7). We suggest this drop delineates the second warmer AW anomaly front downstream of the M1 mooring toward the North Pole. Our estimation shows this spatial feature is not attributable to the AW jet migration across the Eurasian flank of the Lomonosov Ridge because the magnitude of δ here is much smaller than the magnitude of the anomaly. The low magnitude of δ near the North Pole

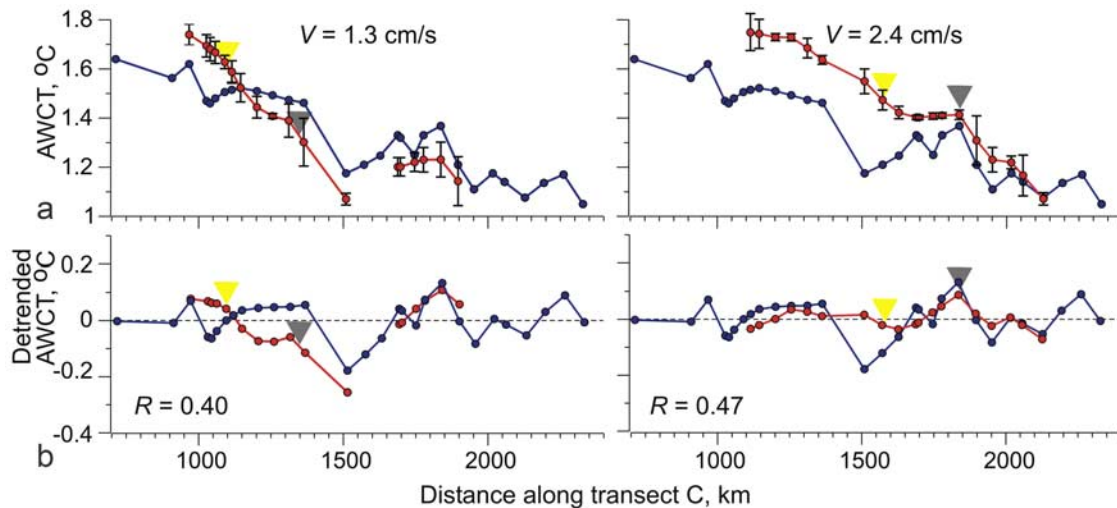


Figure 8. (a) Along-margin AWCT derived from the 2002–2005 M1 mooring time series (red lines) for an AW propagation speed V of (left) 1.3 cm/s and (right) 2.4 cm/s versus the along-margin 2005 AWCT derived from the CTD/XBT transect C (blue lines). See section 6 for details on calculating mooring-derived AWCT and its standard deviations, shown by error bars. (b) Linearly detrended along-margin AWCT. Gray and yellow arrows delineate the along-margin position of the AWCT warmer anomalies recorded at the M1 mooring in February and August 2004, respectively (see also Figure 3). Gaps in the mooring-derived record are due to missing data.

is also confirmed by aerial hydrographic CTD surveys from 2002 to 2006 [see, e.g., *Kikuchi et al.*, 2005].

[27] Farther north, following transect C up to the North Pole, the anomaly does not exceed 0.12°C , remaining comparable with noise δ . The upstream (0–700 km) anomaly magnitude only exceeds the long-term mean cooling over the range of 0–185 km, and only exceeds the noise level over the narrow band of 0–120 km (Figure 7). Note that the δ derived from the 2005 snapshot section intersected the along-margin section C at the most western station roughly perpendicular to C (not shown), confirming the long-term mean δ estimation (Figure 6b).

[28] We delineate two fronts of the AWCT warmer anomalies propagating along the Eurasian flank of the Lomonosov Ridge toward the North Pole. These fronts are delineated along transect C downstream of the M1 mooring at approximately 1510 and 1930 km (Figure 7). The magnitude of anomaly between 1150 and 1400 km is comparable to the amount of noise, δ ; therefore any effort to identify the front by subtracting the anomaly signal would be highly speculative. Identification of an upstream AW warm anomaly front at 200 km also remains unreliable due to insufficient 2005 data coverage.

6. Comparison of the 2005 Along-Margin Transect With the Mooring Record

[29] Distinct patterns of the two warm anomalies observed at the M1 mooring allow us to trace the propagation of mooring-recorded anomalies downstream along the basin margins. Below we estimate the downstream anomaly propagation speed linking the M1 mooring 2002–2005 MMP AWCT record to the 2005 along-margin AWCT section. Our basic goal is to relate the AWCT time series derived from the 2002–2005 M1 mooring MMP record to

the spatial AWCT patterns measured during the 2005 along-margin transect C.

[30] The basic assumption is that the AWCT patterns recorded by the M1 mooring are propagating along-margin downstream without substantial temporal transformation. This assumption implies a simple relationship between the time dimension t and the spatial along-margin dimension L : $L = Vt$, where V is the AW downstream propagation velocity. We also assume that V is constant over the along-margin dimension L ($dV/dL = 0$). First, the AWCT daily time series $T = f(t)$ from the M1 MMP record was smoothed by taking a 7-d running mean. Then we transformed the AWCT time series $T = f(t)$ into along-margin AWCT sections $T = f(L)$ by means of the relationship introduced above between t and L for a range of AW downstream propagation velocity $V = 0.7$ –4.0 cm/s. Finally, the AWCT along-margin sections were 50 km binned to the position of the 2005 along-margin CTD/XBT stations and linearly detrended. Examples of the along-margin AWCT sections derived from the 2002–2005 M1 mooring AWCT time series for $V = 1.3$ and 2.4 cm/s versus the along-margin 2005 CTD/XBT AWCT are shown in Figure 8a. Error bars show the range of AWCT variability over the 50 km bins as estimated by the standard deviation. Detrended sections are shown in Figure 8b.

[31] In order to identify the range of AW downstream propagation velocity V that provides the best match between the detrended AWCT along-margin sections derived from the M1 mooring temperature time series and the 2005 along-margin CTD/XBT section, the V -lagged correlation R between these two sections was computed. The along-margin detrended AWCT sections derived from the M1 mooring for the V range of 0.7–4 cm/s with an increment of 0.1 cm/s were correlated with the AWCT along-margin section derived from the 2005 along-margin CTD/XBT transect. An analysis of the sensitivity of this computed

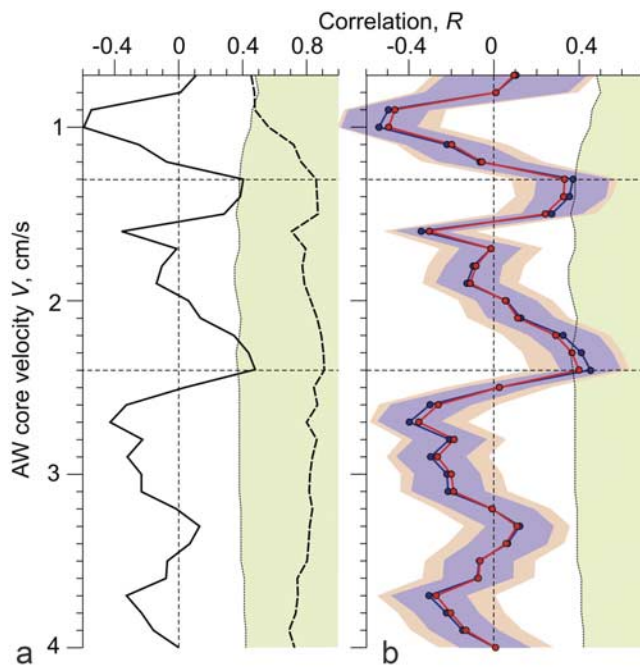


Figure 9. V -lagged correlation R between mooring and CTD/XBT section-derived along-margin AWCT. Green shading shows statistically significant range of correlation at 95% level of confidence. (a) Correlation calculated for original (dashed line) and detrended (solid line) AWCT along-margin data. (b) Correlation between randomly noised series of along-margin AWCT data. Blue and red lines correspond to means of 1,000,000 correlations between data series randomly noised with maximum and minimum AWCT variance rates, respectively (see text for details). The blue and red shaded areas show the range of the resulting correlations at the 95% confidence level for maximum and minimum variances, respectively.

correlation to the noise attributed to cross-margin migration of the AW core was tested by randomization of the correlated data. We added Gaussian noise to the detrended along-margin AWCT section data. For CTD/XBT-derived data, random noise was calculated using the range of climatic mean AWCT standard deviation (δT_i) at the positions of all 2005 along-margin CTD/XBT stations. For mooring-derived data the AWCT variance was attributed to the standard deviation of the AWCT mean calculated over the 50 km range from station position. The resulting 1000 noisy series for both mooring and CTD/XBT-derived AWCT data were employed to calculate the V -lagged correlation R over the V range of 0.7–4 cm/s; this process was repeated 10^6 times. A correlation procedure based on randomization was also applied as an alternative method to identify the statistical significance of the computed correlation.

[32] The V -lagged correlation R between mooring- and CTD/XBT-derived along-margin AWCT sections is shown in Figure 9. Figure 9a identifies two statistically significant (with 95% confidence) best matches between detrended data for the AW propagation velocity of 1.3 cm/s ($R = 0.40$)

and 2.4 cm/s ($R = 0.47$). The V -lagged correlation of AWCT along-margin anomalies (not shown, see section 5.2 for details on calculating AWCT anomalies) exhibits a similar two-peak structure with maxima at 1.3–1.5 and 2.3–2.4 cm/s. Figure 9b shows the mean R of 10^6 correlations that were calculated between randomly noised along-margin data series. R was calculated for both minimum (red line) and maximum (blue line) variance derived from the standard deviations depicted by error bars in Figure 6b and Figure 8a. Shading in Figure 9b shows the range of R variability with 95% confidence. The sensitivity analysis demonstrates the robustness of our conclusions for a V lag of 2.3–2.4 cm/s for the full range of the AWCT variances. The V lag of 1.3 cm/s falls slightly below the range of significance at the 95% level of confidence (Figure 9b). However, the red and blue shading in Figure 9b showing the range of resulting correlation with 95% level of confidence identifies statistically significant correlations (at a 95% confidence level) for the V lags of 1.3–1.5 and 2.2–2.4 cm/s. Summarizing our correlation results, one may conclude that there are two different bands of AW core downstream propagation speeds at 1.3 cm/s and 2.4 cm/s; each of these two different speeds seems to represent an equally good match between the mooring-derived along-margin AWCT section and the 2005 CTD/XBT data.

[33] Here we argue that the slower lag speed of 1.3 cm/s is far less than the lowest estimation of the AW anomaly propagation velocity, and therefore should be rejected. We present two pieces of supporting evidence. Heat is lost as the AW propagates downstream from the M1 mooring (Figure 6). Consequently, the along-margin AWCT derived from the M1 mooring record becomes comparable with AWCT measured during the 2005 CTD/XBT transect C only after adjustment by the rate of along-margin climatic cooling. Without such an adjustment, the AWCT from the M1 mooring record exceeds the AWCT derived from the 2005 along-margin observations. This evidence supports a lag of 2.4 cm/s; a lag of 1.3 cm/s would be supported by the opposite case, if the along-margin AWCT derived from transect C exceeded that revealed from M1 mooring record (Figure 8a).

[34] Furthermore, from the independent data source we demonstrate that the lag of 1.3 cm/s is much slower than the lowest estimation of February 2004 anomaly propagation velocity. The AW warming recorded on transect B in September 2004 (Figure 5b, bottom) has been attributed to the downstream propagation of the AW warmer anomaly which passed the M1 mooring in February 2004 (Figure 3). It took less than 200 d of travel time for this anomaly to reach cross-margin transect B, 385 km downstream of the M1 mooring, yielding a lower estimation of anomaly propagation speed of about 2.2 cm/s. This estimation appears reasonably comparable to the 2.3–2.4 cm/s revealed by our V -lagged correlation analysis. The alternative estimation of 1.3 cm/s is much below this range and therefore has been rejected.

7. The 2000s Warm Atlantic Water Anomaly Spreads Along the Eurasian Basin Margins

[35] Here we compare previous results independently obtained by comparison of the along-margin 2005 AWCT

section with the along-margin AW pre-1990 mean and the 2002–2005 AWCT mooring record. We examine both the along-margin location of the AW anomaly fronts and the anomaly propagation speed. We also compare these independent AW velocity estimations with velocity data from the M1 and M2 moorings, modeling results by *Karcher et al.* [2003], and tracer estimations by *Frank et al.* [1998].

[36] We argue that our results for the downstream anomaly fronts, independently obtained by two different methods, are in reasonable agreement. Assuming the downstream AW anomaly propagation speed of 2.4 cm/s, the AWCT warmer anomaly that had passed the M1 mooring in February 2004 appears to have been located 1151 km downstream by August 2005 (exact travel time is 555 d), i.e., at 1865 km of transect C. The August 2004 M1 mooring AWCT warmer anomaly front was located 758 km downstream in August 2005 (366 d of travel time), i.e., at 1472 km of transect C. These estimations are reasonably close to independent estimates obtained by comparison of 2005 CTD/XBT data with the AW pre-1990 mean (compare 1865 with 1930 km, and 1472 with 1510 km for the first and second anomaly fronts, respectively, Figure 7). Moreover, for the warmer AW front that passed the M1 mooring in August 2004, the estimation based on V -lagged correlation falls within the error range of the first estimation calculated from the spatial uncertainty of front determination by nearby oceanographic stations (Figure 7). In terms of propagation speed, the difference between these two independent estimations is negligible; compare 2.4 cm/s (from V -lagged correlation analysis) with 2.5 ± 0.2 and 2.4 ± 0.1 cm/s (the AW mean for the February and August 2004 fronts, respectively).

[37] The warm anomaly front that passed through Fram Strait into the Nansen Basin in January 2001 [*Schauer et al.*, 2004; *Polyakov et al.*, 2005] is delineated by comparison with the AW long-term mean at 1762 km downstream. This comparison yields an anomaly propagation velocity of 1.2 ± 0.1 cm/s upstream of the M1 mooring. The error range is based on the spatial uncertainty of front determination by nearby oceanographic stations (Figure 7).

[38] There are several pieces of evidence supporting our estimations of the AW anomaly propagation speed. The first comes from comparison of our downstream velocity estimations with the AW core velocity records at moorings M1 and M2. Our estimations are in reasonable agreement with the measured 1.5-year mean AW core speed of 2.2 cm/s from the M1 mooring and the 3.0 cm/s annual mean AW core speed at M2 (Figure 4). Note however that two moorings deployed in 1995–1996 over the Eurasian flank of the Lomonosov Ridge near its junction with the Siberian shelf recorded a higher annual mean AW core velocity of 5.4 cm/s over the Laptev Sea slope, and a lower speed of 1.3 cm/s over the Eurasian flank of the Lomonosov Ridge [*Woodgate et al.*, 2001]. There are no upstream observational data available to verify our anomaly propagation speed estimate of 1.2 cm/s. Although our estimate is speculative, it fits well with previously obtained results: *Polyakov et al.* [2005] determined a propagation speed of 1.5 cm/s for the 1999 Fram Strait anomaly downstream along the Nansen Basin margin to the Laptev Sea.

[39] A second piece of evidence comes from comparison with results of numerical modeling by *Karcher et al.* [2003]. Results of numerical modeling of the 1990s anomaly

propagation estimated a 1.2 cm/s eastward current north of Franz Josef Land, similar to our estimation. *Karcher et al.*'s [2003] estimate of a 2.2 cm/s eastward current along the western Laptev Sea continental margin also agrees well with our estimate of 2.3–2.5 cm/s.

[40] A third piece of evidence comes from comparison with results of tracer analyses by *Frank et al.* [1998]. Using tritium/ ^3He data, *Frank et al.* [1998] estimated the current speed in the core of the Barents Sea AW branch over the Laptev Sea continental slope to be 2.0 cm/s. Assuming the current speed estimated by *Frank et al.* [1998] is valid for the entire AW layer, this compares favorably with our estimation of 2.3–2.5 cm/s.

8. Concluding Remarks

[41] Our analysis suggests that the Arctic Ocean is in transition toward a new, warmer state, with possible implications for an Arctic sea ice cover that is already in a reduced state. Observational data collected over the Eurasian Basin margins show the AW temperature increase since February 2004 lasted 19 months, until the end of the available record in September 2005. Comparison with the thermal equilibrium of 2002–2003 shows a 2005 AW core temperature anomaly of 0.8°C that approaches the magnitude of the anomaly found in the Eurasian Basin in the 1990s.

[42] We argue that the 2005 snapshot of along-margin water properties shows a time history of the along-margin AW boundary current. Our CTD and XBT profiles taken along the Laptev Sea continental slope and the Eurasian flank of the Lomonosov Ridge in August–September 2005 suggest cooling of the AW, with along-margin downstream spreading that differs from the long-term mean pattern. The high degree of similarity between the 2005 snapshot and the AW temperature time series from our upstream mooring allows us to attribute this difference to the downstream propagation of a warmer AW anomaly that was first recorded in the Fram Strait in March 1999, detected farther downstream in the Laptev Sea in February 2004, and measured along the Lomonosov Ridge in August 2005. The anomaly magnitude exceeds the level of pre-1990 mean along-margin cooling and rises above the level of noise attributed to shifting of the AW jet across the basin margins. Anomaly propagation speed along the Amundsen Basin margin has been estimated by two independent methods as 2.3–2.5 cm/s. Data collected using our current meters, results of numerical modeling by *Karcher et al.* [2003], and tracer tritium/ ^3He studies by *Frank et al.* [1998] corroborate these estimations.

[43] Our data suggest the 2004 AW temperature signal propagates along the Amundsen Basin margins downstream of the northern Laptev Sea with a speed of ~ 2 cm/s. This seemingly contradicts the much smaller estimate of upstream advection along the Nansen Basin continental margin that has been recently reported by *Polyakov et al.* [2005]. The reason for the increasing advection speed far from the source of the AW inflow is a matter of debate. A consideration of this contradiction suggests that it is hard to be precise on advection timescales with the data currently available. There are no long-term current observations over the Eurasian Basin continental margin between Franz Josef

Land and the northern Laptev Sea. We speculate that the AW boundary current is tightly locked to the complex bathymetry in the northern Kara Sea, where it has been recorded that the topographically trapped AW flow follows two deep canyons connecting the inner Kara Sea to the Nansen Basin [Schauer *et al.*, 2002]. Although our data are not sufficient to allow us to draw final conclusions, it is evident that the time taken for the AW to traverse the Amundsen Basin continental margin is at least 5.5 months, implying an advective speed of ~ 2 cm/s.

[44] There are also some caveats to our analysis. We assume throughout that the AW flows as a topographically controlled boundary current several hundred kilometers wide, and does not cross the Amundsen Basin by traveling straight from Cape Arkticheskiy to the shelf junction with the Lomonosov Ridge.

[45] Ongoing and future observations in this region will clarify our findings. They are also expected to capture continuous warming of the AW layer along the Eurasian Basin continental margins due to continuing influx of warmer AW through Fram Strait and the downstream along-margin propagation of AW toward the North Pole where we anticipate rapid AW warming will occur in 2007.

[46] **Acknowledgments.** This research is a part of ongoing NOAA and NSF-funded IARC Program “Nansen and Amundsen Basins Observational System” (NABOS). S.K. acknowledges funding through the NAVO grant N41756-05-M-6433. I.P. and V.I. thank the Frontier Research System for Global Change for financial support. The M2 mooring is maintained thanks to funding through the Network of Centres of Excellence of Canada: ArcticNet. The research cruise aboard the R/V *Akademik Fedorov* was funded by the Russian Ministry for Hydrometeorology (Roshydromet).

References

- Aagaard, K. (1989), A synthesis of the Arctic Ocean circulation, *Rapp. P. V. Reun. Cons. Int. Explor. Mer.*, 188, 11–22.
- Boyd, T. J., M. Steel, R. D. Muench, and J. T. Gunn (2002), Partial recovery of the Arctic Ocean halocline, *Geophys. Res. Lett.*, 29(14), 1657, doi:10.1029/2001GL014047.
- Carmack, E., K. Aagaard, J. Swift, R. Perkin, F. McLaughlin, R. Macdonald, P. Jones, J. Smith, K. Ellis, and L. Kilius (1997), Changes in temperature and tracer distributions within the Arctic Ocean: Results from the 1994 Arctic Ocean Section, *Deep Sea Res., Part II*, 44, 1487–1502, doi:10.1016/S0967-0645(97)00056-8.
- Dmitrenko, I. A., I. V. Polyakov, S. A. Kirillov, L. A. Timokhov, H. L. Simmons, V. V. Ivanov, and D. Walsh (2006), Seasonal variability of Atlantic water on the continental slope of the Laptev Sea during 2002–2004, *Earth Planet. Sci. Lett.*, 244(3–4), 735–743, doi:10.1016/j.epsl.2006.01.067.
- Environmental Working Group (1997), *Joint U.S.–Russian Atlas of the Arctic Ocean* [CD-ROM], Natl. Snow and Ice Data Cent., Boulder, Colo.
- Frank, M., W. M. Smethie, and R. Bayer (1998), Investigation of subsurface water flow along the continental margin of the Eurasian Basin using the transient tracers tritium, ^3He , and CFCs, *J. Geophys. Res.*, 103(C13), 30,773–30,792, doi:10.1029/1998JC900003.
- Karcher, M. J., R. Gerdes, F. Kauker, and C. Koberle (2003), Arctic warming: Evolution and spreading of the 1990s warm event in the Nordic seas and the Arctic Ocean, *J. Geophys. Res.*, 108(C2), 3034, doi:10.1029/2001JC001265.
- Kikuchi, T., J. Inoue, and J. H. Morison (2005), Temperature difference across the Lomonosov Ridge: Implications for the Atlantic Water circulation in the Arctic Ocean, *Geophys. Res. Lett.*, 32, L20604, doi:10.1029/2005GL023982.
- Morison, J. H., *et al.* (2002), North Pole environmental observatory delivers early results, *Eos Trans. AGU*, 83(33), 357, doi:10.1029/2002EO000259.
- Morison, J., M. Steele, T. Kikuchi, K. Falkner, and W. Smethie (2006), Relaxation of central Arctic Ocean hydrography to pre-1990s climatology, *Geophys. Res. Lett.*, 33, L17604, doi:10.1029/2006GL026826.
- Polyakov, I., D. Walsh, I. Dmitrenko, R. Colony, J. Hutchings, L. Timokhov, M. Johnson, and E. Carmack (2003a), A long-term circulation and water mass monitoring program for the Arctic Ocean, *Eos Trans. AGU*, 84(30), 281, doi:10.1029/2003EO300001.
- Polyakov, I., D. Walsh, I. Dmitrenko, R. L. Colony, and L. A. Timokhov (2003b), Arctic Ocean variability derived from historical observations, *Geophys. Res. Lett.*, 30(6), 1298, doi:10.1029/2002GL016441.
- Polyakov, I. V., G. V. Alekseev, L. A. Timokhov, U. S. Bhatt, R. L. Colony, H. L. Simmons, D. Walsh, J. E. Walsh, and V. F. Zakharov (2004), Variability of the intermediate Atlantic Water of the Arctic Ocean over the last 100 years, *J. Clim.*, 17(23), 4485–4497, doi:10.1175/JCLI-3224.1.
- Polyakov, I., *et al.* (2005), One more step toward a warmer Arctic, *Geophys. Res. Lett.*, 32(17), L17605, doi:10.1029/2005GL023740.
- Quadfasel, D., A. Sy, D. Wells, and A. Tunik (1991), Warming in the Arctic, *Nature*, 350, 385, doi:10.1038/350385a0.
- Rudels, B., E. P. Jones, L. G. Anderson, and G. Kattner (1994), On the intermediate depth waters of the Arctic Ocean, in *The Polar Oceans and Their Role in Shaping the Global Environment: The Nansen Centennial Volume*, *Geophys. Monogr. Ser.*, vol. 85, edited by O. M. Johannessen, R. D. Muench, and J. E. Overland, pp. 33–46, AGU, Washington, D. C.
- Rudels, B., G. Bjork, R. D. Muench, and U. Schauer (1999), Double-diffusive layering in the Eurasian Basin of the Arctic Ocean, *J. Mar. Syst.*, 21, 3–27, doi:10.1016/S0924-7963(99)00003-2.
- Rudels, B., R. Meyer, E. Fahrbach, V. Ivanov, S. Osterhus, D. Quadfasel, U. Schauer, V. Tverberg, and R. A. Woodgate (2000), Water mass distribution in Fram Strait and Yermak Plateau in summer 1997, *Ann. Geophys.*, 18, 687–705, doi:10.1007/s00585-000-0687-5.
- Schauer, U., B. Rudels, E. P. Jones, L. G. Anderson, R. D. Muench, G. Bjork, J. H. Swift, V. Ivanov, and A.-M. Larsson (2002), Confluence and redistribution of Atlantic water in the Nansen, Amundsen and Makarov basins, *Ann. Geophys.*, 20(2), 257–273.
- Schauer, U., E. Fahrbach, S. Osterhus, and G. Rohardt (2004), Arctic warming through the Fram Strait—Oceanic heat transport from three years of measurements, *J. Geophys. Res.*, 109(C6), C06026, doi:10.1029/2003JC001823.
- Swift, J. H., E. P. Jones, K. Aagaard, E. C. Carmack, M. Hingston, R. W. MacDonald, F. A. McLaughlin, and R. G. Perkin (1997), Waters of the Makarov and Canada basins, *Deep Sea Res., Part II*, 44(8), 1503–1529, doi:10.1016/S0967-0645(97)00055-6.
- Timofeev, V. T. (1957), Atlantic waters in the Arctic basin (in Russian), *Probl. Arkt. Antarkt.*, 2, 41–52.
- Woodgate, R. A., K. Aagaard, R. D. Muench, J. Gunn, G. Bjork, B. Rudels, A. T. Roach, and U. Schauer (2001), The Arctic Ocean boundary current along the Eurasian slope and the adjacent Lomonosov Ridge: Water mass properties, transports and transformations from moored instruments, *Deep Sea Res., Part I*, 48, 1757–1792, doi:10.1016/S0967-0637(00)00091-1.
- Woodgate, R. A., K. Aagaard, J. H. Swift, W. M. Smethie Jr., and K. K. Falkner (2007), Atlantic water circulation over the Mendeleev Ridge and Chukchi Borderland from thermohaline intrusions and water mass properties, *J. Geophys. Res.*, 112, C02005, doi:10.1029/2005JC003416.

I. A. Dmitrenko, Leibniz Institute of Marine Sciences, University of Kiel (IFM-GEOMAR), Wischhofstr. 1-3, Build. 4, D-24148 Kiel, Germany. (idmitrenko@ifm-geomar.de)

I. E. Frolov, S. A. Kirillov, V. T. Sokolov, and L. A. Timokhov, Arctic and Antarctic Research Institute, 38 Bering Street, St. Petersburg 199397, Russia. (frolov@aari.nw.ru; dia@aari.nw.ru; svt@aari.nw.ru; ltim@aari.nw.ru)

V. V. Ivanov, I. V. Polyakov, and H. L. Simmons, International Arctic Research Center, University of Alaska Fairbanks, 930 Koyukuk Drive, Fairbanks, AK 99775-7340, USA. (vivanov@iarc.uaf.edu; igor@iarc.uaf.edu; hsimmons@iarc.uaf.edu)

D. Walsh, Pacific Tsunami Warning Center, 91-270 Fort Weaver Road, Ewa Beach, HI 96706, USA. (david.walsh@noaa.gov)